Near-deterministic creation of universal cluster states with probabilistic Bell measurements and three-qubit resource states

Hussain A. Zaidi, Chris Dawson, Peter van Loock, and Terry Rudolph

Phys. Rev. A **91**, 042301 — Published 1 April 2015

DOI: 10.1103/PhysRevA.91.042301

Near-deterministic creation of universal cluster states with probabilistic Bell measurements and 3-qubit resource states

Hussain A. Zaidi,[1,2,*] Chris Dawson,[3] Peter van Loock,[4] and Terry Rudolph[5,†]

[1]*Department of Physics, University of Virginia, 382 McCormick Road, Charlottesville, Virginia 22904*
[2]*Department of Biochemistry and Molecular Biology, University of Virginia, 1340 Jefferson Park Avenue, Charlottesville, Virginia 22908, USA*
[3]*Quantitative Brokers, 2 Queen Caroline Street, London, W6 9DX, UK*
[4]*Institute of Physics, Johannes-Gutenberg Universität Mainz, Staudingerweg 7, 55128 Mainz, Germany*
[5]*Controlled Quantum Dynamics Theory Group, Imperial College London, Prince Consort Road, London SW7 2BW, UK*

We develop a scheme for generating a universal qubit cluster state using probabilistic Bell measurements without the need for feed-forward. Borrowing ideas from percolation theory we numerically show that using unambiguous Bell measurements that succeed with 75% success probability one could build a cluster state with an underlying pyrochlore geometry such that the probability of having a spanning cluster approaches unity in the limit of infinite lattice size. The initial resources required for the generation of a universal state in our protocol are 3-qubit cluster states that are within experimental reach and are a minimal resource for a Bell-measurement-based percolation proposal. Since single and multi-photon losses can be detected in Bell measurements, our protocol raises the prospect of a fully error-robust scheme.

PACS numbers: 42.50.Ex, 03.67.Lx

I. INTRODUCTION

A realistic blueprint for a quantum computer will have to contend with non-deterministic quantum operations that succeed only probabilistically. It is known that efficient quantum information processing is possible using linear-optical elements, feed-forward, and photon number resolving detectors (PNRDs), where the measurements subject to feed-forward induce the required non-linear transformations probabilistically [1]. This insight was later applied to the case of one-way quantum computation [2] by using probabilistic linear-optical quantum operations along with feed-forward to create universal quantum resource states [3, 4] on which quantum algorithms could be implemented by suitably choosing "easy" local measurements. A major technological challenge in the above proposals is the requirement of feed-forward which adds to the resource requirements of quantum memories.

An important step in devising proposals without feedforward was presented in [5, 6]. These proposals used the ideas of percolation theory to show that a percolated lattice could be created without feedforward or long-time memories, which could then be renormalized to a universal cluster state, e.g. one with the geometry of a square lattice. Specifically, Ref. [6] dealt with creating a pyrochlore lattice starting with 4-qubit cluster states using Type-I fusion gate [4] that succeeded with 50% success probability and consumed one qubit upon application. The downside of using a Type-I fusion gate is that it is not robust to photon losses, making the application of the ideas of [5, 6] practically demanding.

On another note, Bell measurements form an important part of quantum computation and communication protocols [1, 7–9]. Without feed-forward, ancillary photons or non-linear quantum operations, the success probability of a Bell measurement is bounded by 50% [10]. Recently, a few proposals came out [11–13] that increased the success probability of unambiguous Bell measurements past 50% without feedforward by using Bell pairs, squeezers or single photons, along with linear optical elements and PNRDs. Ref. [11] describes a scheme for unambiguous Bell measurement that has a success probability of 75% with ancillae Bell pairs. Ref [13] uses single photon ancilla for 75% success probability, and Ref [12] uses squeezing for a success probability of more than 62% without any ancilla modes. These schemes allow for the detection of either single-photon or multi-photon losses, which makes them appealing from the perspective of error correction.

While the use of Bell measurements in entanglement distribution has been studied in the past [8, 14], here we deal with the specific question of using probabilistic unambiguous Bell measurements to create large quantum resource states that suffice for universal quantum computation, with the specific focus of minimizing the size of the initial resources needed. We propose creating a percolated pyrochlore lattice starting with 3-qubit cluster states. We assume that these initial resource states along with either Bell pairs or single photons (depending on the chosen Bell measurement scheme) are available on demand. Since Bell measurements consume two qubits upon application, 3-qubit initial states are a minimal resource for generating large cluster states. Other schemes that use 3-qubit resources or single photons for generating universal states in an error-robust way without relying on ideas of percolation theory [15, 16] require considerable feed-forward. The lack of feed-forward in

*Electronic address: haz4z@virginia.edu
†Electronic address: rudolph@imperial.ac.uk

percolation based protocols makes these protocols well-suited for integrated photonics architectures where the primary source of loss is expected to be photonic switching [17, 18]. Background details on percolation theory in the context of generating universal resource states can be found in [5, 6].

We begin by describing the use of probabilistic Bell measurements to "fuse" cluster states (i.e. to generate entanglement between two unentangled cluster states). We then show how 3-qubit cluster states can be fused to form a large universal quantum state using Bell measurements that succeed with 75% probability. Specifically, we choose the underlying geometry of our cluster state to be that of a pyrochlore lattice with random deletions of bonds (entanglement) and vertices (qubits) due to the probabilistic nature of Bell measurements. Next, we provide numerical evidence demonstrating that we are above the percolation threshold for our pyrochlore lattice, i.e. for 75%-success probability Bell measurements, the probability of having a spanning cluster in one direction approaches unity as the size of the lattice is increased. This spanning cluster is a general graph (not a linear cluster state) that can be renormalized to a universal state. Finally, we look at the scaling behavior of the scheme as a function of the size of the lattice in three dimensions. That is, we estimate the required lattice size in the transverse directions such that the probability of having a spanning cluster in the lateral direction is above 90%. We mention that either of the schemes for Bell measurements [11, 13] could be used in our protocol since they use resource states that are smaller than 3 qubits.

II. BELL MEASUREMENTS FOR FUSION

Consider two cluster states that we want to fuse into one as presented in Fig. [1]. Qubit $1'$ has a Hadamard rotation applied to it before measurement. $\mathcal{A}$, $\mathcal{B}$, $\mathcal{C}$, and $\mathcal{D}$ represent the neighbours of qubits i, 1, $1'$, and j, respectively. For any chosen neighbours (i and j) of measured qubits 1 and $1'$, Fig. [1] depicts the effect on i and j for a successful (i.e., unambiguous) Bell measurement.

The analysis that leads to Fig. [1] follows closely the treatment presented in [19]. In passing we mention that the application of the Hadamard rotation to one of the measured qubits allows us to create cluster-like bonds between the neighbours of the measured qubits instead of GHZ-like bonds as was the case for the treatment presented in [19]. This is important for creating a lattice with a pyrochlore underlying geometry.

Pick a qubit i that neighbours qubit 1 and qubit j that neighbours qubit $1'$ as shown in Fig. [1] of the main text. We apply a Bell measurement on qubits 1 and $1'$. Qubit 1 could have multiple neighbours in addition to i, and similarly qubit $1'$ could neighbour multiple qubits in addition to j. The stabilizers [20] for the qubits (S) can

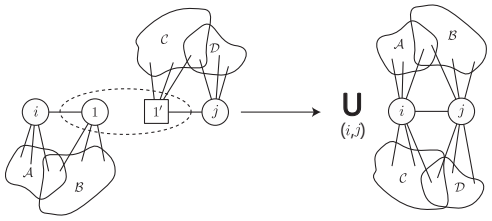

FIG. 1: The effect of a successful Bell measurement (measuring qubits 1 and $1'$). A square node represents a polarization qubit with a Hadamard applied to it, while a dashed oblong around two qubits denotes a Bell measurement. The italicized labels $\mathcal{A}$, $\mathcal{B}$, $\mathcal{C}$, and $\mathcal{D}$ denote graphs for which the products of Pauli Z operators are represented as A, B, C, and D, respectively, in the text. The arguments presented in the text apply to *all* neighbours of the measured qubits, and hence, other neighbours inherit entanglement just as is shown for the qubits i and j. Hence, $\bigcup$ represents the union of all graphs over all possible combinations of neighbours of qubit 1 (i) and neighbours of qubit $1'$ (j).

be written as

$$S_i = AX_iZ_1 \quad , \quad S_1 = BX_1Z_i \tag{1a}$$
$$S_j = Z_{1'}X_jD \quad , \quad S_{1'} = X_{1'}Z_jC, \tag{1b}$$

where A, B, C, and D signify products of Pauli Z operators for neighbours of i, 1, $1'$, and j, respectively. Applying the hadamard on $1'$ results in

$$S_i = AX_iZ_1 \quad , \quad S_1 = BX_1Z_i \tag{2a}$$
$$S_j = X_{1'}X_jD \quad , \quad S_{1'} = Z_{1'}Z_jC. \tag{2b}$$

Performing a Bell measurement on qubits 1 and $1'$ implies that our projectors are, among others, $X_1X_{1'}$ and $Z_1Z_{1'}$. For the measured state, the two new stabilizers that commute with the projectors are

$$\bar{S}_i = S_iS_{1'} = AX_iZ_jC \tag{3a}$$
$$\bar{S}_j = S_iS_j = BZ_iX_jD. \tag{3b}$$

This implies that there is a cluster-like bond between the qubits i and j. The qubit i inherits all its neighbours alongwith the neighbours of $1'$, j inherits all its neighbours along with the neighbours of 1. This analysis holds for all qubits i and j that are neighbors of 1 and $1'$, respectively. It also holds for other projectors in the Bell basis up to local unitary operations. Hence, the resultant cluster state is a graph union over possible ways of picking i and j as shown in Fig. [1].

An important question is what happens when a Bell measurement results in an ambiguous output. Two arbitrary cluster states can always be represented by $|A\rangle = |0\rangle|\xi\rangle + |1\rangle|\xi'\rangle$, and $|B\rangle = |0\rangle|\Xi\rangle + |1\rangle|\Xi'\rangle$, where the primes denote that the neighbours of the first qubit have a Pauli Z operation applied to them. Applying a

Hadamard on the first qubit of $|B\rangle$, and writing the target qubits in the Bell basis yields

$$\begin{aligned}|A\rangle|B\rangle \sim &\left(|\phi^+\rangle + |\phi^-\rangle + |\psi^+\rangle - |\psi^-\rangle\right)|\xi\rangle|\Xi\rangle \\ &- \left(|\phi^+\rangle + |\phi^-\rangle - |\psi^+\rangle + |\psi^-\rangle\right)|\xi\rangle|\Xi'\rangle \\ &+ \left(|\phi^+\rangle - |\phi^-\rangle + |\psi^+\rangle + |\psi^-\rangle\right)|\xi'\rangle|\Xi\rangle \\ &+ \left(|\phi^+\rangle - |\phi^-\rangle - |\psi^+\rangle - |\psi^-\rangle\right)|\xi'\rangle|\Xi'\rangle \quad (4)\end{aligned}$$

Notice that when the Bell measurement results in an unambiguous output, we get $|\xi\rangle(|\Xi\rangle + |\Xi'\rangle) + |\xi'\rangle(|\Xi\rangle - |\Xi'\rangle)$ as the conditional state for the remaining qubits (up to local unitaries), which is indeed entangled between the qubits of $|A\rangle$ and those of $|B\rangle$. To analyze the failure mechanism, say that our Bell measurement fails to distinguish between $|\phi^+\rangle$ and $|\phi^-\rangle$, which is indeed a probabilistic failure event in [11, 13]. Further, assume that the magnitude of the coefficient of the ambiguous output is the same for both the inputs, which is also the case for [11, 13]. Then the output looks like $|\xi\rangle(|\Xi\rangle - |\Xi'\rangle)$ or $|\xi'\rangle(|\Xi\rangle - |\Xi'\rangle)$. This failure behavior means different consequences for different input graph states. The two case that are relevant for us are that of a 3-qubit triangle cluster input and a 3-qubit chain cluster input.

A 3-qubit triangular cluster is given by $\sim |0\rangle(|0+\rangle + |1-\rangle) + |1\rangle(|0-\rangle - |1+\rangle)$. Hence, upon failing to fuse two triangular clusters we are left with a pair of Bell states up to local rotations, as shown in Fig. [2]. On the other hand, if we are trying to fuse a 3-qubit cluster chain, $\sim |0\rangle(|0+\rangle + |1-\rangle) + |1\rangle(|0+\rangle - |1-\rangle)$ (with Hadamard applied to one qubit), with another arbitrary state, then upon failure we are left with just $|1-\rangle$ for the qubits of the chain, i.e. the qubits of the chain are disentangled from each other. Notice that in both the above cases, the outcome for the cluster on which we do not apply a Hadamard is just that the measured qubit is destroyed and the rest of the graph stays intact up to local unitary operations.

III. PYROCHLORE LATTICE SCHEME

The above success and failure mechanisms suffice to construct a percolated pyrochlore lattice. First, we fuse 3-qubit triangular clusters to form tetrahedra as shown in Fig. [2].

This step succeeds with a probability of 75% owing to the success probability of Bell measurements. Next, we take the outputs of the first step (e.g. two tetrahedra), and fuse them together using a 3-qubit chain, as shown in Fig. [3].

The 3-qubit chain acts as an intermediary in fusing two tetrahedra and producing the correct geometry of the resulting lattice that we desire. This step succeeds only when both the Bell measurements succeed, which happens with a theoretical probability of 56.25%.

The above two steps, outlined in Figs. [2] and [3], can be repeated multiple times to create a full-fledged

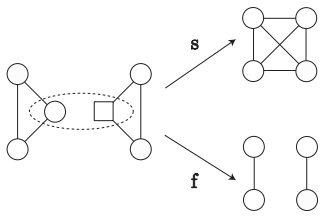

FIG. 2: Fusing two triangular clusters with Bell measurements results in a 4-qubit tetrahedron upon success (denoted by "s"). Failure of the measurement (denoted by "f", and implying an ambiguous measurement outcome) results in two Bell pairs (up to local operations), which can still be used in subsequent fusions shown later.

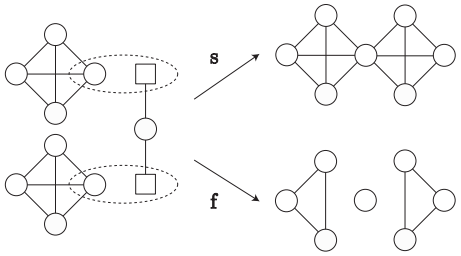

FIG. 3: The 3-qubit chain is used as an intermediary to fuse two tetrahedra together to form a "bowtie". Since there are two Bell measurements involved, the theoretical success probability of this step is 56.25%.

pyrochlore lattice of the desired size. Fig. [4] outlines the repeated fusion process in order to create a larger pyrochlore lattice.

It is important to emphasize that the entire process can be accomplished ballistically in a single shot since all the measurements commute with each other. The entanglement structure of the cluster state only depends on the failure or success of the individual measurements, not their sequence. For example, if the fusion of a pair of triangular clusters failed, we'd be left with a pair of Bell pairs, which we'd use for further fusions. In that sense, the figures only show representative possible outcomes; the outcome in an experiment will be statistical.

Refs. [5, 6] deal with the process of renormalization in depth. Here, we briefly state that renormalization of the pyrochlore lattice percolated in this manner can be accomplished by considering (polynomially many) hypothetical cubic blocks of some chosen size overlaid on the pyrochlore lattice. By measuring out suitable qubits in the Z basis we can ensure spanning paths between the desired faces of the block as well as renormalize the qubits in the blocks to single qubits. As the number of blocks grows there is an increasing probability that one or more will fail to be connected, but this can be dealt with by simply increasing the block sizes. Because such an increase in size improves the spanning probability expo-

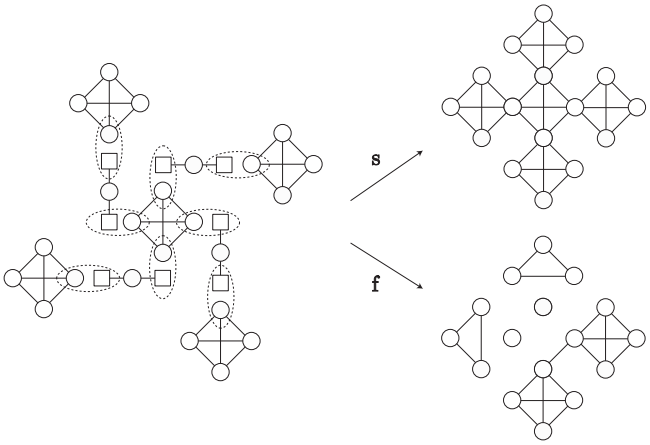

FIG. 4: 3-qubit chains are used as intermediaries to fuse five tetrahedra together. The failure event is an example of what happens when the pair of fusions at the top and the top-left fail.

nentially, we can conclude that a polynomial sized computation is feasible with polynomial resources.

IV. NUMERICAL SIMULATION

Given that the above process cannot be mapped on to a simple vertex percolation or edge percolation problem, no analytical method for analyzing the percolation threshold for our scheme is known. Hence, we resort to simulating our scheme numerically in C++ [21]. First, a fully connected $n_x \times n_y \times n_z$ pyrochlore lattice was built by translating the cell shown in Fig.[5(a),(b)] n_x, n_y, and n_z times in the x, y and z directions, respectively. Hence, adding a unit cell corresponds to adding 26 qubits to our simulation. Next, 25% of the tetrahedra were reduced to two disconnected "lines", simulating the failure outcome of Fig.[2]. Finally, 56% of the vertices were disconnected simulating the failure outcome of Fig. [3]. Fig. [5 (c),(d)] show the effect of the two steps on a $1 \times 1 \times 1$ pyrochlore lattice (i.e. a pyrochlore "unit cell" for our purposes).

As seen in Fig. [6], the probability of having a spanning cluster in the x-direction approaches unity as the success probability of Bell measurement is increased from 65% to 90% (for a sample size of 200 trials) and illustrates that the fusion probability of 75% is above the percolation threshold.

To accurately estimate the percolation threshold, we simulated our protocol on lattice sizes of $12 \times 12 \times 12$, $14 \times 14 \times 14$, and $16 \times 16 \times 16$, the results of which are shown in Fig. [7]. The figure shows that the percolation threshold is between fusion probabilities of 69.5% and 70.0%, which is lower than the 75% theoretical fusion success probability.

From an experimental point of view, we would like to know how big the underlying lattice needs to be in the y and z directions so that the probability of having a spanning cluster in the x direction is above some experimental threshold, say, 90%. To answer this question, we ran numerical simulations for various values of n_x, n_y and n_z. The results of these simulations are shown in Table [I].

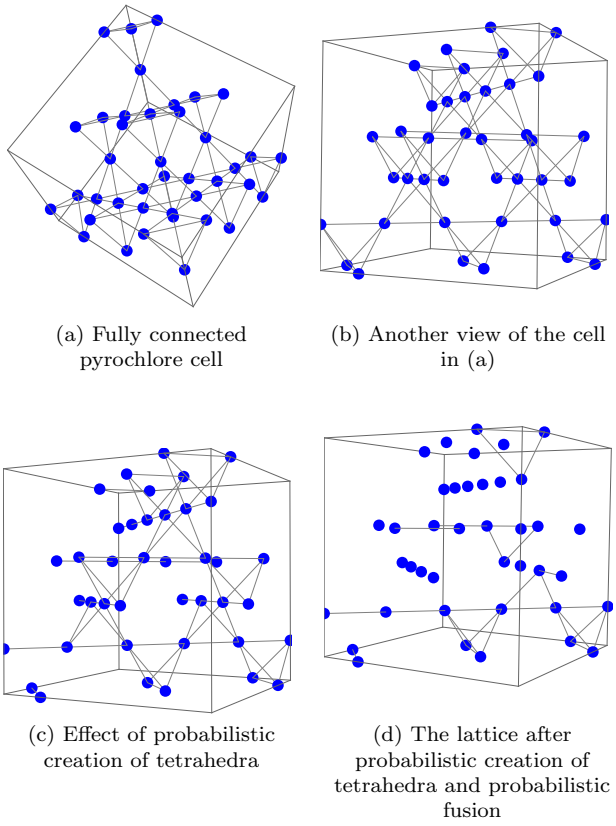

(a) Fully connected pyrochlore cell

(b) Another view of the cell in (a)

(c) Effect of probabilistic creation of tetrahedra

(d) The lattice after probabilistic creation of tetrahedra and probabilistic fusion

FIG. 5: (Color online) Simulation of spanning-cluster generation using 3-qubit cluster states. Figure (d) shows a representative outcome on a unit cell, while figures (a) and (b) show a fully connected pyrochlore cell, which is what the protocol would produce if Bell measurements were deterministic.

As mentioned before, adding a unit cell corresponds to adding 26 qubits, because of which our scaling results give us a course resolution in the scaling of the lattice size. Nonetheless, the simulations show that the size of the lattice can be kept to a few unit cells in the z direction (roughly 3) to be above the 90% threshold for any required spanning length in the x direction if the size in y is of the order of the size in x. That is important for potential experiments since in optical-chip experiments it is desirable to have either a planar or an almost planar lattice [17].

V. DISCUSSION AND FUTURE DIRECTIONS

We have proposed creating a percolated pyrochlore cluster using probabilistic Bell measurements. By doing so, we have brought down the initial resources re-

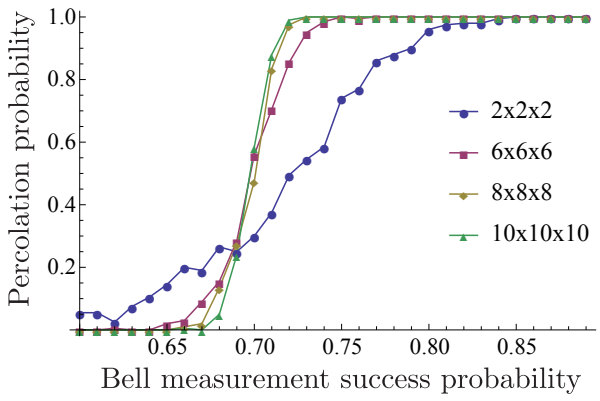

FIG. 6: (Color online) Percolation probability versus the success probability of Bell measurement for various pyrochlore lattice sizes. Each lattice size was sampled 200 times.

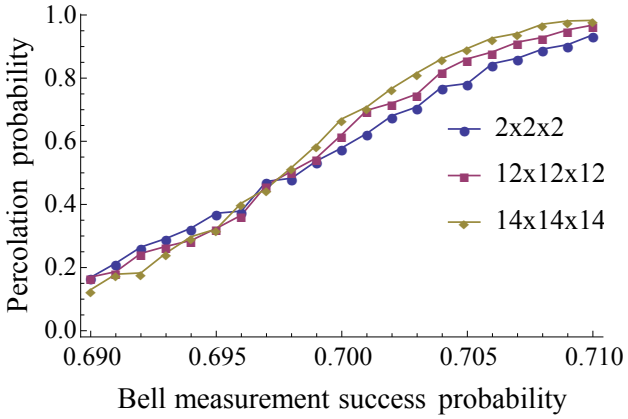

FIG. 7: (Color online) Percolation probability versus the success probability of Bell measurement. Large number of trials (1000), large lattice sizes, and a small step size in the fusion probability (0.001) allow us to pin-point the percolation threshold to be between 69.5% and 70%.

quired to generate universal cluster states using a percolation approach from 4-qubit to 3-qubit cluster states; 3 qubits being the minimal required size for generating universal cluster states using Bell measurements. Our proposal creates near-planar cluster states, which is of particular interest in optical-chip architectures of quantum computation. Even though we assumed that the success probability of Bell measurements was 75%, the percolation threshold for our scheme is between 69% and 70% as shown in Fig. [7], which implies that our scheme should scale well in the presence of experimental errors. The two largest errors in photonics are systematic imperfections (interferometers that are misaligned) and photon losses, plus some small amount of Pauli error from any active elements (primarily switches) [17, 18]. The repeatability of systematic errors makes them relatively benign, and the fact that losses are always ultimately detected means that correcting for them is considerably easier than for unknown Pauli error. Finding a way to combat all sources of error simultaneously in this architecture is ongoing work [16].

TABLE I: Scaling of lattice size in y and z as a function of the length in x. We set 90% as the minimum probability threshold for having a spanning path. The success probality was calculated from 200 samples for each value of n_x, n_y and n_z

n_x	n_y	n_z	Lattice size	Success Probability (%)
4	4	4	1444	96
5	5	3	1680	91
6	6	3	2352	91
7	7	3	3136	92
8	7	3	3556	93
9	7	3	3976	90
10	8	3	4984	94
11	8	3	5460	94
12	9	3	6636	96
13	9	3	7168	92
14	9	3	7700	92
15	9	3	8232	91

VI. ACKNOWLEDGEMENTS

H.Z. was supported by US AFOSR Grant No. FA9550-11-1-0297. He is thankful to the Institute of Physics at the University of Mainz (where part of this work was completed) for their hospitality. PVL was supported by QuOReP (BMBF) and HIPERCOM (ERA-Net CHIST-ERA). TR supported by the by the Vienna Science and Technology Fund (WWTF, grant ICT12-041) and the Army Research Office (ARO) grant No. W911NF-14-1-0133. The authors are thankful to Mercedes-Gimeno Segovia for helpful discussions.

[1] E. Knill, R. Laflamme, and G. Milburn, Nature **409**, 46 (2001).
[2] R. Raussendorf and H. Briegel, Phys. Rev. Lett. **86**, 5188 (2001).
[3] M. Nielsen, Phys. Rev. Lett. **93**, 040503 (2004).
[4] D. Browne and T. Rudolph, Phys. Rev. Lett. **95**, 010501 (2005).
[5] K. Kieling, T. Rudolph, and J. Eisert, Phys. Rev. Lett.

99, 130501 (2007).
[6] K. Kieling and J. Eisert, Quantum and Semi-classical Percolation and Breakdown in Disordered Solids pp. 287–319 (2008).
[7] K. Mattle, H. Weinfurter, P. Kwiat, and A. Zeilinger, Phys. Rev. Lett. **76**, 4656 (1996).
[8] L. Duan, M. Lukin, J. Cirac, and P. Zoller, Nature **414**, 413 (2001).
[9] D. Gottesman and I. Chuang, Nature **402**, 390 (1999).
[10] J. Calsamiglia and N. Lütkenhaus, Appl. Phys. B **72**, 67 (2001).
[11] W. Grice, Phys. Rev. A **84**, 042331 (2011).
[12] H. Zaidi and P. van Loock, Phys. Rev. Lett. **110**, 260501 (2013).
[13] F. Ewert and P. van Loock, Phys. Rev. Lett. **113**, 140403 (2014).
[14] S. Bose, V. Vedral, and P. Knight, Phys. Rev. A **57**, 822 (1998).
[15] M. Varnava, D. Browne, and T. Rudolph, New Journal of Physics **9**, 203 (2007).
[16] M. Varnava, D. Browne, and T. Rudolph, Phys. Rev. Lett. **100**, 060502 (2008).
[17] J. Matthews, A. Politi, A. Stefanov, and J. O'Brien, Nat. Photonics **3**, 346 (2009).
[18] D. Berry and H. Wiseman, Nat. Photonics **3**, 317 (2009).
[19] P. Kok and B. Lovett, *Introduction to optical quantum information processing* (Cambridge University Press, Cambridge, UK, 2010).
[20] D. Browne and H. Briegel, pre-print (2006), arXiv:quant-ph/0603226v2.
[21] C. Dawson and H. Zaidi, *C++ code for calculating percolation threshold for 2d and 3d lattices*, https://github.com/cmdawson/percolation/tree/arXiv (2014).